Received: 4 December 2024 | Revised: 4 March 2025 | Accepted: 21 April 2025

DOI: 10.1111/jace.20614

Journal of the American Ceramic Society

RESEARCH ARTICLE

Surface characterization of sodium silicate glasses after initial water interaction

Katsuaki Miyatani[1,2] | **Shin-ichi Amma**[3] | **Lu Deng**[4,5] | **Jayani Kalahe**[4] | **Mari Morioka**[2] | **Michinori Suehara**[2] | **Madoka Ono**[6] | **Shingo Urata**[2] | **Jincheng Du**[4] | **Ken-ichi Fukui**[1]

[1]Department of Materials Engineering Science, Graduate School of Engineering Science, Osaka University, Toyonaka, Osaka, Japan

[2]Innovative Technology Laboratories, AGC Inc., Yokohama-shi, Kanagawa, Japan

[3]Materials Integration Laboratories, AGC Inc., Yokohama-shi, Kanagawa, Japan

[4]Department of Materials Science and Engineering, University of North Texas, Denton, Texas, USA

[5]Shanghai Institute of Optics and Fine Mechanics, Chinese Academy of Science, Shanghai, China

[6]Department of Applied Physics, Tohoku University, Sendai, Miyagi, Japan

Correspondence
Katsuaki Miyatani, Department of Materials Engineering Science, Graduate School of Engineering Science, Osaka University, machikaneyama, Toyonaka, Osaka 560–8531, Japan.
Email: katsuaki.miyatani@agc.com

Funding information
Institute for Nanoscience Design, Osaka University

Abstract

The corrosion behavior of sodium silicate glass in water may be understood by clarifying the fundamental processes of interface reactions. We investigated the reaction mechanism of the glass surfaces in contact with water for just an immediate dipping up to 1 h later, using x-ray photoelectron spectroscopy. Silanol formation due to ion exchange of sodium with hydrogen from water was observed from 0 to 30 s, similar to previously reported molecular dynamics simulations. However, the amount of silanol groups decreased after the formation reaction owing to the dehydration of excess silanol groups generated by the initial reactions, thereby promoting the re-formation of siloxane networks at the glass surface. The generated siloxane network was relatively stable for 30 min owing to their rather rigid network. The silanol group concentration increased gradually at the surface after 30 min, owing to a deficiency of dissolved sodium ions. Thereafter, the sodium ions attracted to the negatively charged glass surface gradually left the surface, resulting in an increase of silanol groups when the glass–water reaction proceeded. These observations of the glass–water reaction over a short period provide insight for improving the durability of sodium silicate glass products and developing efficient polishing and cleaning procedures for glass fabrication.

KEYWORDS
corrosion/corrosion resistance, glass, interfaces

1 | INTRODUCTION

Silicate glasses are typically transparent and exhibit high mechanical strength and corrosion resistance. Therefore, multicomponent silicate glasses are widely used as windows in architecture and automobiles, substrates in display devices,[1] and cover glasses of smartphones.[2] For the latter, a smooth surface with precise control of roughness is required.[3, 4] These and other emerging applications require more precise control of the surface roughness and flatness of glass substrates; thus, a better understanding of the glass–water reaction is needed, as exposure to water or

aqueous solutions commonly occurs during the processing or application of these glass materials.[3, 4]

To satisfy these requirements, glass substrates are usually lapped, polished, and then cleaned,[5] during which the glass substrate is repeatedly dipped in water or aqueous solutions. Therefore, understanding the solid–liquid interface reactions occurring at the interface between glass and water is extremely important for designing the fabrication processes of glass products.

Silicate glass corrosion is governed by several interrelated and often overlapping processes, including ion exchange, hydration, hydrolysis, condensation, and precipitation.[6–8] On the other hand, the silica-rich, hydrated porous gel layer on the surface, which is formed by the initial dissolution of silicate or borosilicate glass, can serve as a passivation layer and limit the further diffusion of water molecules to the reaction front.[8] The exact mechanism of the formation of this gel layer and the manner in which it limits ion transport has still been unclear; however, it is acknowledged that the hydrated interfacial gel layer is formed by one of two processes: by hydrolysis of the silicate network followed by condensation or repolymerization, or by network dissolution followed by precipitation.[7] The transport-limiting effect is probably enabled by self-reorganization of the gel layer that leads to pore closures or the nano-confinement effect that limits water transport in the gel layer.[6] The above results were obtained using advanced experimental characterizations and sophisticated atomistic simulations.[6, 9] However, these studies investigated the long-term (from several years to hundreds to thousands of years) corrosion of glass, where the residual rate of the glass is the main concern. By contrast, investigations limited to the period immediately after the initial exposure of glass to water often focus on the initial dissolution rate (from the solution concentration of the dissolved species); however, the nature of the glass surface is often not carefully examined immediately after the initial immersion.

When we focus on the sodium silicate glass, a target material in this manuscript, in water, previous studies indicated the ion exchange of surface sodium cations by protons to form surface silanol,[10–14] and siloxane formation by dehydration condensation reaction of the two silanol groups.[11, 15, 16] An x-ray photoelectron spectroscopy (XPS) study after dipping a sodium silicate glass in aqueous solutions of various pHs for 24 h showed the pH-dependent changes of surface Na/Si ratio and the peak shift of Na 1s.[17] But the timescale of such changes and their relation with the surface states of the sodium silicate glass are not clear.

The short-term behavior is significant in many industrial applications.[18] For example, during glass processing, glass substrates are exposed to water for a relatively short time, that is, from a few seconds to a few minutes. However, few studies have investigated the corrosion mechanisms of sodium silicate glass surfaces within this short timescale. Therefore, this study focuses on the reaction behavior at the glass–water interface at the initial stage.

TABLE 1 Composition and density of the sodium silicate glass used in corrosion experiments.

Target compositions (mol.%)		Measured compositions (mol.%)		Density (wt.%)
SiO_2	Na_2O	SiO_2	Na_2O	
77.3	22.7	80.6	19.4	2.402

In addition to experimental investigations, molecular dynamics (MD) simulations, particularly those with reactive potentials, have been used to study water reactions on glass surfaces, usually within a short period of up to tens of nanoseconds. For instance, reactions between water and sodium silicates,[19–22] sodium aluminosilicates,[23–26] and magnesium aluminosilicate[27] have been investigated using reactive MD simulations. Furthermore, reactive MD simulations have been used to investigate glass polishing processes.[28–33] The simulation results provide a valuable resource for comparison with experimental observations performed on short timescales, such as those focused on in this work. Reactive MD simulation studies on the water–glass reactions of a series of sodium silicate glasses[19, 20] have demonstrated that the protons in water are immediately exchanged with sodium ions at the glass surface when the glass interacts with water, and silanol groups are formed on the glass surfaces. Simultaneously, these sodium ions are removed from the glass by ion exchange and diffuse into the bulk water region. Thereafter, the protons of the silanol groups are exchanged with sodium ions located inside the glass; thus, the amount of silanol groups increases in the subsurface or bulk of the glass. Following silanol formation inside the glass, water slowly diffuses into the glass via the proton transfer and the ion exchange. Motivated by these insights from reactive MD simulations, we analyzed the changes of chemical states of glass surfaces, such as variations in the amount of sodium and silanol groups on the glass surfaces, using XPS during a short timescale (from a few seconds to up to 1 h) after dipping the sodium silicate glass plates in water.

2 | EXPERIMENTAL PROCEDURES

2.1 | Sample Preparation

The composition of the sodium silicate glass used in our experiments was 80.6 mol.% SiO_2 and 19.4 mol.% Na_2O with a glass density of 2.402 g/cm^3 (Table 1).

The glass was prepared using the melt-quenching procedure.[34] The composition and density of the glass were analyzed using XRF and the Archimedes method, respectively. The annealed glass was cut into plates with dimensions of 50 mm × 50 mm × 1 mm. The glass substrate surface was then polished using a polishing pad (FPK550, Fujibo Ehime Inc.) and colloidal silica slurry (Compol80, Fujimi Inc.) to create a mirrored surface. Polishing was performed at a fixed plate rotation speed of 40 rpm and a polishing load of 98 g/cm^2 for 15 min using FAM12B (SpeedFAM Co. Ltd.). The polished glass substrate was cleaned in pure water and dried under a stream of dry air.

Thereafter, the glass substrate was scribed in air to make glass plates of dimensions 10 mm × 10 mm, which were further cut into two pieces (5 mm × 10 mm) to use the cleaved surface for evaluation. The scribed glass substrate was dipped in 500 mL of pure water and left still for the desired duration and dried under a stream of dry air. Dipping times of 5, 15, 30, 60, and 180 s were used to observe any variations of the surface state with time. In addition, the samples dipped for longer durations (up to 60 min) were examined for comparison. A glass sample and pure water were replaced for each experiment. Negligible change of pH was detected before and after the glass dipping due to sufficient volume of water.

2.2 | X-ray photoelectron spectroscopy (XPS) analysis

Surface analysis was performed via XPS using an AXIS Nova (KRATOS high-speed limited) to identify changes in the surface composition of the glass before and after dipping in pure water. The x-ray source was Al-$K\alpha$, and the voltage and current of the x-ray source were 15 kV and 10 mA, respectively. The energy step, dwell time, and energy analyzer were 0.1 eV, 600 ms, and 10 eV, respectively. The measurement was performed within a 100 μ m × 100 μ m area. The analytical chamber base pressure ranged from 1×10^{-6} to 8×10^{-7} Pa. Three areas were measured per sample to confirm the reproducibility of the XPS measurements. In general, the signal depth was 1–10 nm from the surface. The data analysis of the spectra was performed using OriginPro 2021 software (OriginLab Corporation). After removing the background using the Shirley method,[35] areas of the spectra were calculated to estimate composition ratios. The error in the compositional ratio due to the spectral area fitting was estimated to be less than 15%. State analysis was also performed using OriginPro 2021. The C 1s spectral line was standardized to 285.0 eV, and the Na 1s, O 1s, and Si 2p spectra were adjusted to this energy.

3 | RESULTS

3.1 | X-ray photoelectron spectroscopy spectra before and after dipping into water

The cleaved glass surfaces were analyzed using XPS in the narrow scan mode to identify C 1s, Na 2s, Si 2p, and O 1s. The Na 2s, Si 2p, and O 1s spectra are shown in Figure 1. Standardization of the peak intensities was performed using the Si 2p spectra.

The Na 2s spectra of the glass, before and after immersion in water, are shown on the left side of Figure 1. The height of the XPS peak decreases markedly within the first 5 s of dipping, indicating that the sodium ions left the surface immediately after the glass was dipped in water. The peak intensity continues to decrease over time; however, the reduction in the peak height is more gradual after 15 s, indicating that sodium ion leaching is a fast process that occurs mainly within the first 10–15 s of contact with water. The Si 2p spectra, before and after dipping in water, are shown in the center of Figure 1. The Si 2p spectrum of the glass remains unchanged by the glass–water interaction. The O 1s spectra of the glass, before and after dipping in water, are shown on the right side of Figure 1. The highest energy peak at 536.0 eV can be attributed to the emission of the Na KLL Auger electrons. The intermediate binding energy peak (532 and 533 eV) and the lowest binding energy peak (529 and 530 eV) can be assigned to the emission from the bridging oxygen (BO) and the non-bridging oxygen (NBO), respectively.[36] A broad shoulder in the O 1s spectrum at approximately 530 eV decreases in intensity with time. Because this shoulder peak corresponds to the binding energy of the NBO, it is expected to decrease in the initial stage of the glass–water reaction. This is due to fast sodium ion leaching and repolymerization of the silanol groups, which decreases the fraction of NBO on the top surface. Notably, all peak positions shift toward the higher energy side after 30 s. These chemical shifts are attributed to a decrease in basicity due to the leaching of sodium cations.[37]

3.2 | Amount of sodium at the glass surface

The amount of Na (C_{Na}) was quantitatively evaluated by measuring the area of the Na 2s peak (Figure 2). Three points were measured, and the average values are plotted in this figure as filled circles, together with an error bar, which indicates the maximum and minimum values of the three data points.

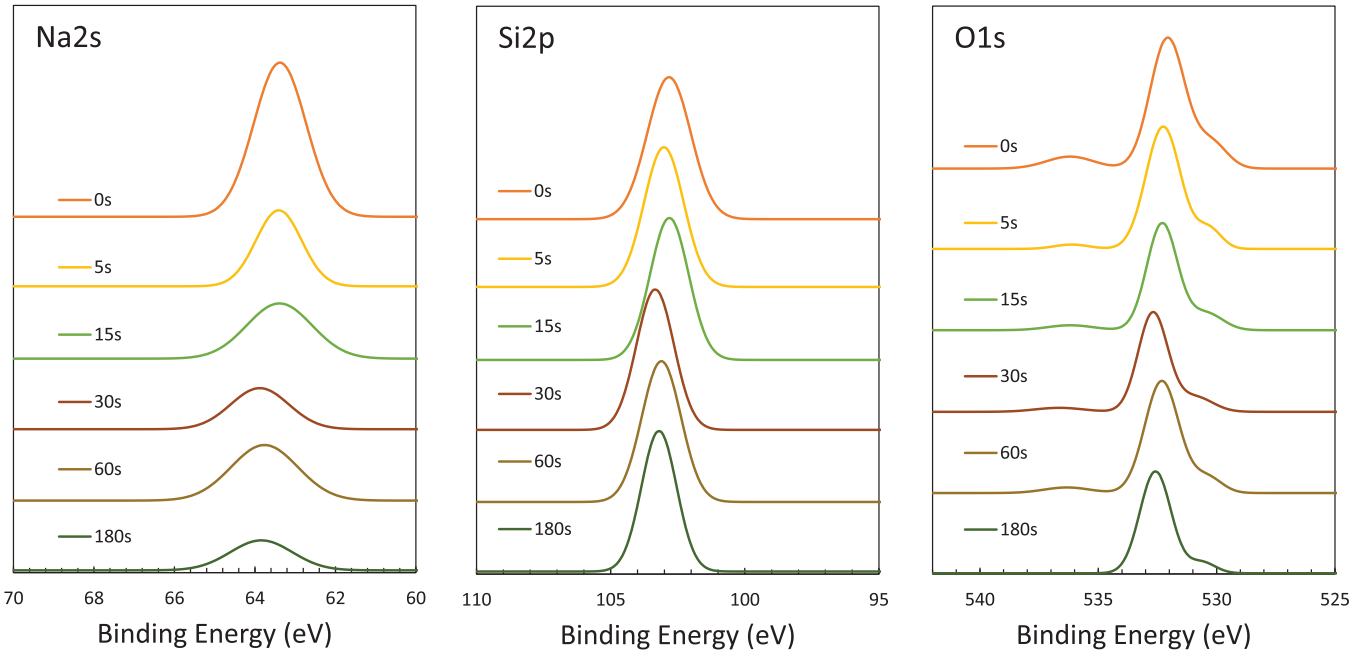

FIGURE 1 X-ray photoelectron spectroscopy spectra of the cleaved surface of a sodium silicate glass after dipping in water for 0, 5, 15, 30, 60, and 180 s, from the top to the bottom.

Figure 2A shows the change in sodium concentration after 200 s of dipping in water. As qualitatively noted above, C_{Na} immediately decreased to approximately 70% of the initial value by 5 s after dipping. Following the initial reaction, the C_{Na} gradually decreased to approximately half that of its initial concentration after 180 s. After the initial rapid leaching, the sodium leaching rate decreased gradually up to 60 min (Figure 2B).

The concentration of Na drops markedly at approximately 30 s, indicating that the reaction mechanisms might be different in the early stage (before 30 s) and the later stages of the glass–water reaction. A very slow reaction rate in the later stage may suggest that the water resistance of the glass surface is once improved by the removal of a certain amount of sodium atoms from the surface, followed by the formation of a silica-rich gel layer, which serves as a diffusion barrier of water molecules to the inner reaction front.

3.3 | State analysis of O 1s

Thereafter, the oxygen species were classified using the O 1s spectrum. Figure 3 displays the spectra obtained before being dipped in water and after 15 and 180 s. The O 1s spectrum usually exhibits a main peak and a broad Na KLL peak.[36] The two peaks indicate that oxygen atoms in the sodium silicate glass may be classified into BO, possessing two siloxane bonds, and NBO, which is bound to only one silicon atom.[36] NBO includes oxygen in ≡ Si–OH and ≡ Si–O–Na.[36] In addition, the spectra may also include water molecules diffusing into the glass.[38] In Figure 3, the raw data of the O 1s spectrum are drawn with a gray line, and Gaussian distributions corresponding to BO, NBO, and water oxygen are drawn in red, blue, and green, respectively. The Na KLL spectra are shown in orange. The accumulated spectrum from the classified spectra confirms the fitting accuracy and is shown using black dots.

The oxygen apparently originating from water was not detected before dipping in water (Figure 3A) and even after 15 s of dipping (Figure 3B). The broad Na KLL peak was apparently decreased by 15 s dipping and slowly decreased further by 180 s dipping, corresponding to the change of the Na 2s peak. After a longer reaction with water for 180 s, a small peak corresponding to oxygen of water appeared at around 535 eV. In the main peak, the portion of the NBO peak decreased by longer dipping into water.

The atomic ratios of BO, NBO, and oxygen in water were determined from the O 1s spectra. The variation in the amount of NBO (C_{NBO}) with dipping time is shown in Figure 4. Figure 4A shows that C_{NBO} monotonically decreased as the early stage up to 180 s dipped. But longer dipping, up to 60 min, did not increase C_{NBO} (Figure 4B).

According to the previous MD simulations,[19, 20] a sodium ion interacting with NBO forming ≡Si–O–Na at the glass surface is released into water as a result of ion exchange with protons, which results in the formation of

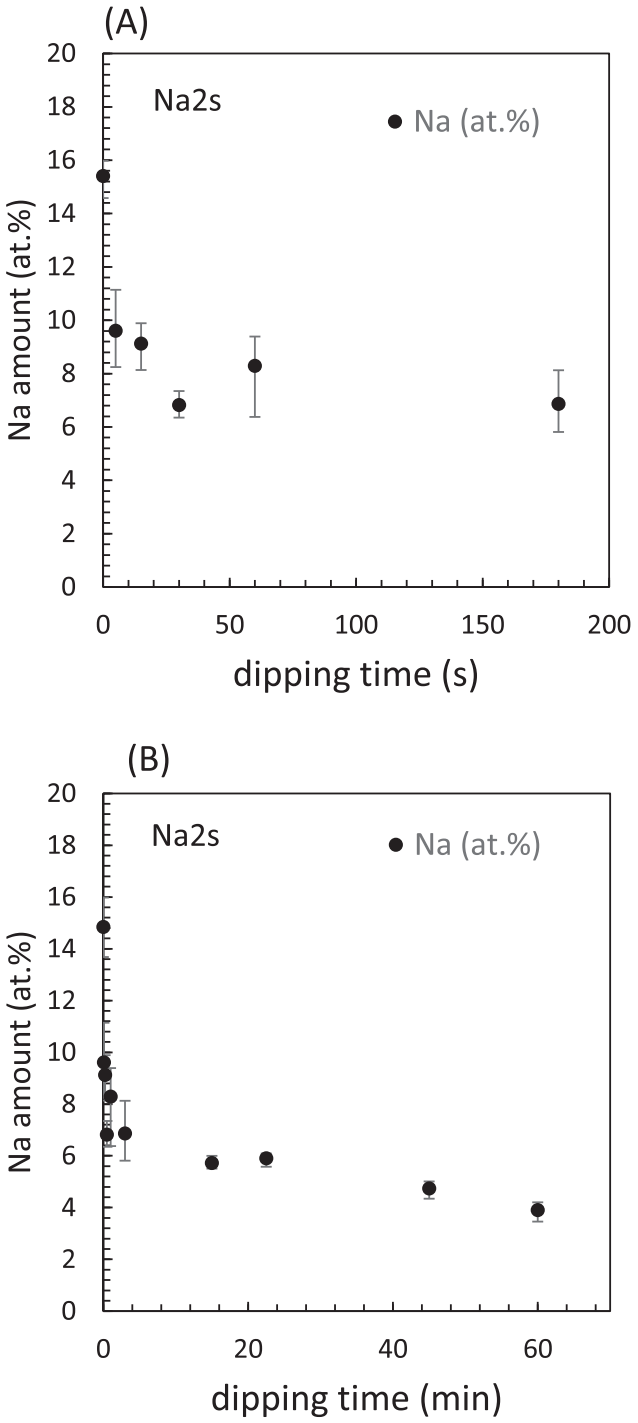

FIGURE 2 Variation in the amount of sodium at the sodium silicate glass surface with dipping time in water, estimated by x-ray photoelectron spectroscopy analysis. Dipping time duration: (A) 0–180 s, (B) 0–60 min.

≡Si–OH. This reaction did not affect C_{NBO}. However, the changes in C_{Na} (shown in Figure 2) and those of C_{NBO} (shown in Figure 4) cannot be explained by this process, indicating that reactions other than ion exchange probably occur on the glass surface when sodium silicate glass reacts with water.

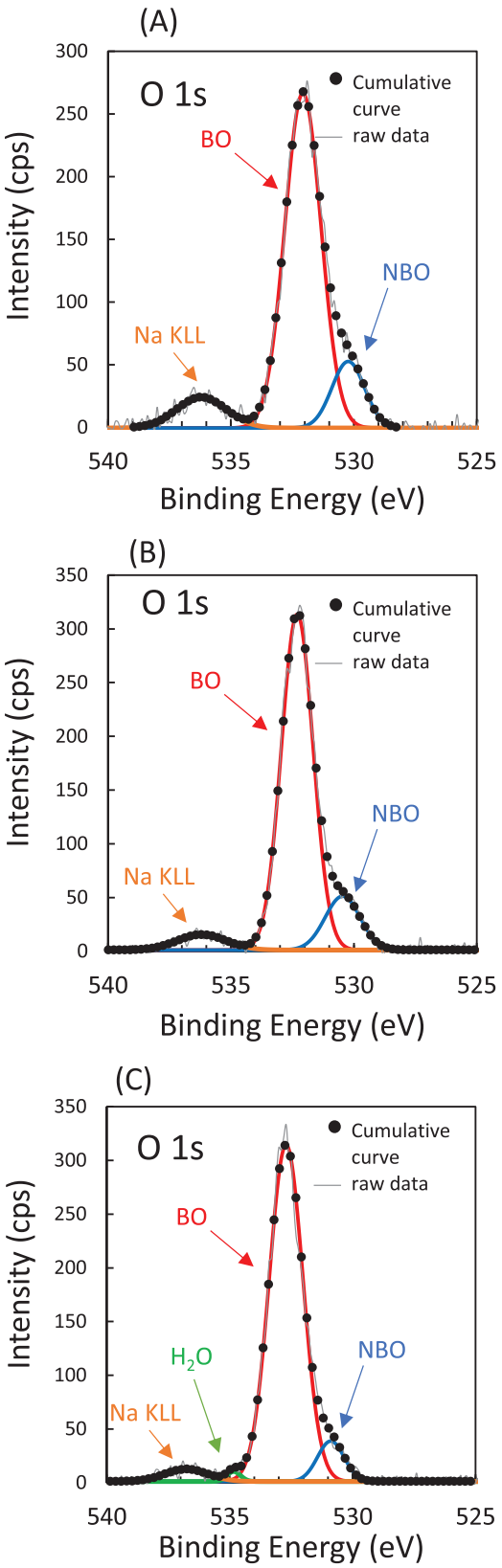

FIGURE 3 O 1s State analysis of sodium silicate glass after dipping into water for (A) 0 s (before dipping), (B) 15 s, and (C) 180 s.

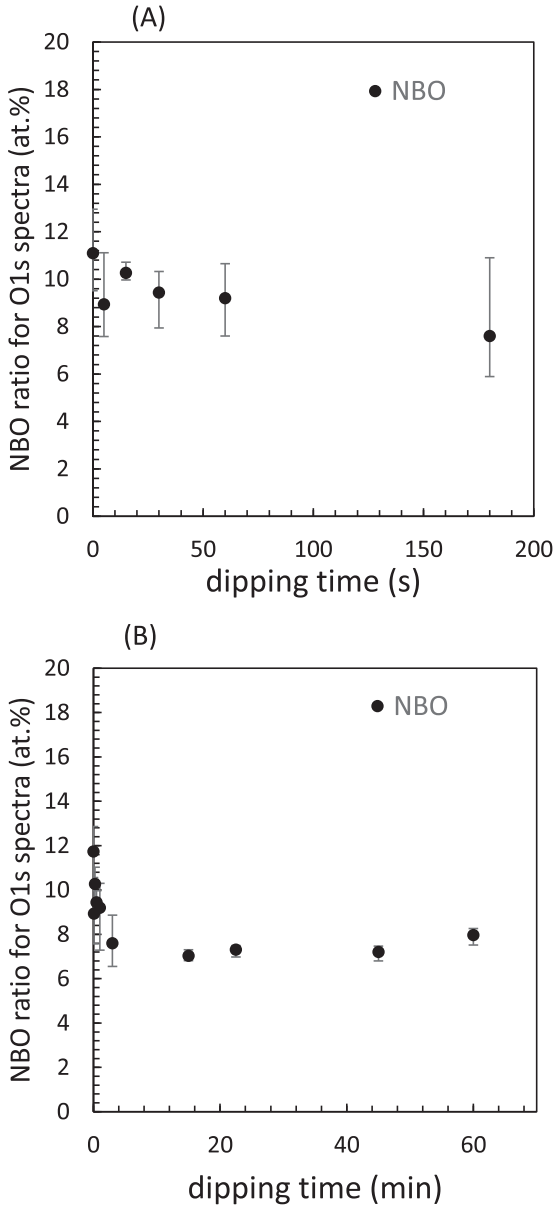

FIGURE 4 Variation of the ratio of non-bridging oxygen at the sodium silicate glass surface with dipping time in water estimated by x-ray photoelectron spectroscopy (XPS) analysis. Dipping time duration: (A) 0–180 s, (B) 0–60 min.

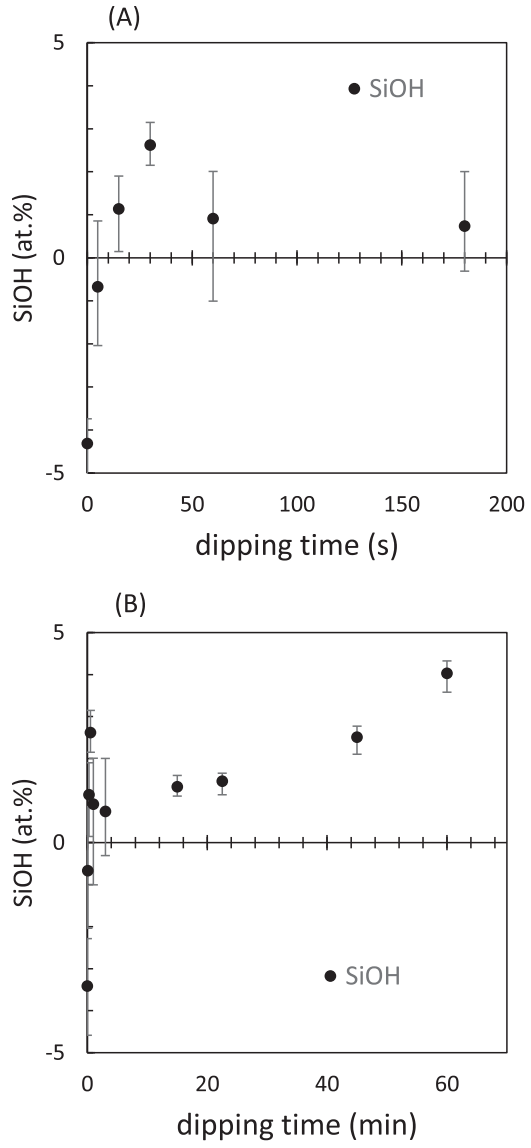

FIGURE 5 Change in the amount of silanol groups with duration of dipping in water, estimated using Equation (1). Dipping duration time: (A) 0–180 s, (B) 0–60 min.

4 | DISCUSSION

In the sodium silicate glass, BO corresponds to siloxane-bonded oxygen, whereas NBO corresponds to ≡Si–OH or ≡Si–O–Na.[32] By using the value of C_{NBO} and CNa determined by the XPS analysis, the amount of silanol group (C_{SiOH}) can be calculated as

$$C_{SiOH} = C_{NBO} - C_{Na} \quad (1)$$

Then, the variation estimated for C_{SiOH} with dipping time is shown in Figure 5. It should be noted that the calculated C_{SiOH} value becomes negative because, according to the XPS measurements, C_{Na} is greater than C_{NBO} initially. This might be because the negatively charged glass surface attracts sodium ions during the XPS measurement, which results in a higher sodium concentration at the surface. Therefore, in this discussion, we focus only on the trend in the change in concentration instead of on the absolute values.

As shown in Figure 5A, C_{SiOH} increases from the initial value until 30 s after being dipped in water. Because C_{Na} rapidly decreased in this early reaction stage, as shown in Figure 2A, it is inferred that protons occupied the sodium coordination site in the vicinity of the NBO as a result of ion exchange. This observation is consistent with the

previous MD simulations,[19, 20] which demonstrated that a water molecule, when it comes close to the NBO site at the surface of sodium silicate glasses, dissociates into a proton and hydroxyl group pair; thereafter, the proton exchanges its position with a sodium ion bound to an NBO at the glass surface to form a silanol group. The reaction can be described as follows:

$$\equiv Si - O - Na + H_2O \rightarrow \equiv Si - OH + Na^+ + OH^- \quad (2)$$

The notable increase in C_{SiOH} during the early reaction stage corresponds to an ion-exchange reaction with water, as observed by atomistic simulations.[19, 20] The timescale of the atomistic simulation was within a short period of 3 ns, which is considerably different from that used in this study.

In this study, C_{SiOH} started to decrease after 30 s, contrary to the prediction of the MD simulations.[19, 20] This is due to the timescale difference. The time accessed in the MD simulation was significantly short (several nanoseconds); hence, the simulation results agreed only with the initial stage below 30 s, in which an increase is observed in C_{SiOH} (Figure 5A). There are two possible explanations for the decrease in the concentration of the silanol groups after 30 s. One is that a proton in a silanol group ($\equiv$Si–$[OH]_{Surface}$) diffuses further into the bulk of the glass, and it replaces a sodium ion located in the subsurface of the glass via the ion-exchange reaction that was observed in the MD simulations[19, 20]:

$$\equiv Si - OH_{surface} + Si - O - Na_{bulk} \rightarrow \equiv Si - O - Na_{surface} + Si - OH_{bulk} \quad (3)$$

This secondary reaction consumes Si–OH and decreases C_{SiOH} if the reaction rate in Equation (3) exceeds that of Equation (2). Another possible reason is the polymerization reaction between two silanol groups located at nearby sites on the glass surface:

$$\equiv Si - OH + HO - Si \equiv \rightarrow \equiv Si - O - Si \equiv + H_2O \quad (4)$$

According to the time variation of C_{Na}, shown in Figure 2, the sodium concentration decreases monotonically, in contrast to that of C_{SiOH}. This implies that the reaction shown in Equation (3) does not contribute to the decrease in C_{SiOH} within 30–60 s. Therefore, it is expected that the excess silanol groups, which are generated by the rapid reaction between the NBO at the glass surface and water molecules, recombine to form siloxane linkages via the condensation reaction, as described in Equation (4).

This hypothesis is explained using schematic diagrams in Figure 6. Figure 6A shows the initial states at the cleaved glass surface, where many sodium ions are bound to the NBO. Immediately after being dipped in water, the sodium ions bonded to the NBO at the glass surface leached out to the bulk water region, accompanied by occupation of the site with protons from water molecules to form silanol groups, as shown in Figure 6B. Because this ion-exchange reaction with the cleaved glass surface is very fast, an excess amount of silanol groups is temporally formed on the glass surface. Subsequently, the excess silanol groups located near each other are polymerized to form siloxane linkages, and thereby C_{SiOH} decreases. In other words, as the network modifier, sodium ions leave the glass surface, a siloxane network is formed at the glass surface via the reactions shown in Equations (2)–(4). Consequently, a silica-rich gel layer forms and serves as a thin barrier against water diffusion at the sodium silicate glass–water interface.

The dehydration reaction was also demonstrated by reactive MD simulations[19, 20]; however, a decrease in C_{SiOH} was not observed, maybe due to the accessible timescale differences. The MD simulations could investigate the reactions over a few nanoseconds, which corresponds to the very beginning of the early reaction stage; thus, there might be no excess silanol groups in the glass model owing to the time limitation of atomistic simulations.

After 180 s, C_{SiOH} increases again at a rate much lower than that in the early reaction stage. The stable hydration of the glass surface may be governed by ion exchange between water molecules and two types of sodium ions: One remains at the glass surface, and the other diffuses from the glass subsurface owing to the ion-exchange reaction described in Equation (3). This diffusion phenomenon of sodium ions is slowly seen to proceed from glass surface because C_{Na} already reduced by about half comparing initial state.

The concentration of the silanol group on the glass surface is also affected by the sodium concentration. Once silanol groups form at the surface, some of the protons partially dissociate from the silanol groups in water, as shown in Figure 7B.[36] As a result, the glass surface becomes negatively charged, attracting sodium ions to the surface (Figure 7C). This sodium ion attachment to the glass–water interface was also observed in MD simulations of silicate[6] and aluminosilicate glasses.[24, 39] In addition, zeta potential measurements have confirmed that the surface of silicate glass is negatively charged.[40]

Figure 8 schematically illustrates the sodium concentration at the glass–water interface. According to Figure 2A, C_{Na} at the surface after 60 s is approximately half that of the initial concentration, indicating that the remaining half is in the water phase. Nevertheless, some of the sodium ions,

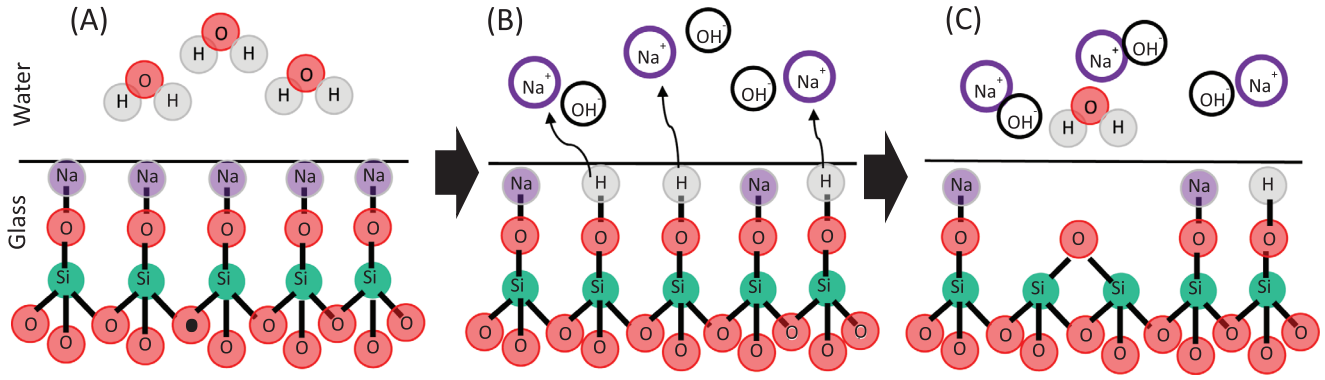

FIGURE 6 Schematic illustration representing reaction processes near the surface of sodium silicate glass immediately after being dipped in water: (A) 0; (B) 5–30; (C) 30–60 s.

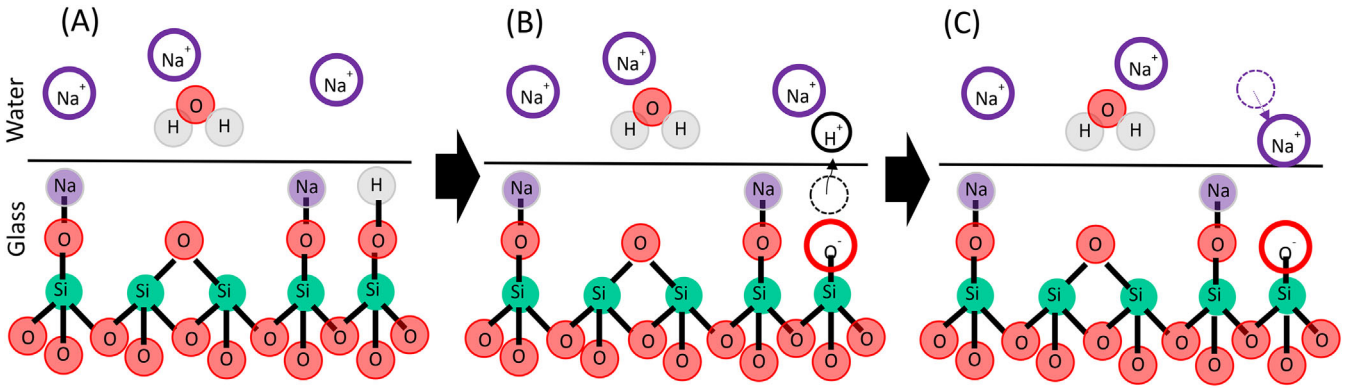

FIGURE 7 Schematic illustration representing reaction processes after 60 s: (A) after ion exchange between sodium ion and water hydrogen (the same condition applies to Figure 6C); (B) a proton being released from the silanol group; (C) a sodium ion approaches the negatively charged glass surface.

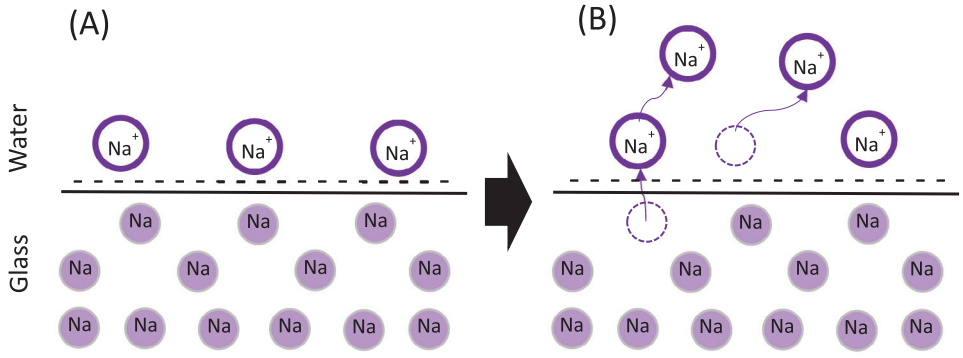

FIGURE 8 Schematic illustration of the sodium concentration near the glass–water interface by (A) 20 to (B) 60 min dipping.

which have diffused into water, might remain close to the glass surface due to electrostatic interaction with the negatively charged glass surface. However, the sodium ions, bound to the glass surface, gradually diffuse into water to compensate for the gradient of sodium concentration in the water phase. In addition, an increase in C_{SiOH} during the later stage (Figure 5B) might decrease the zeta potential of the glass surface; the decrease in the zeta potential reduces the binding energy required to attract sodium ions that are located near the surface. Therefore, sodium ions at the glass surface are gradually leached out to the water region, as shown in Figure 2B.

5 | CONCLUSIONS

The surface state of the bulk sodium silicate glass, $(SiO_2)_{80.6}(Na_2O)_{19.4}$, was quantitatively analyzed using XPS measurements immediately after short time range (from 5 s to 60 min) of dipping in water. These results were compared with those obtained from reactive MD simulations investigating reactions at glass–water interfaces.[14, 15] Using XPS measurements, the concentrations and binding energies of Si, Na, and O, as well as the contributions of BO, NBO, and Si–OH species, were evaluated as a function of time. The following conclusions could be made:

After 5 s, a rapid decrease in the sodium concentration was observed at the glass surface. By contrast, the number of NBO did not decrease significantly. Consequently, the number of silanol groups increased rapidly. These observations made within a short period were consistent with the MD simulation results, although the timescales were different.

From 5 to 30 s, the silanol concentration continued to increase. By contrast, from 30 to 180 s, the number of silanol groups decreased, indicating that the siloxane network was recovered by dehydration reactions between nearby silanol groups. This self-healing phenomenon was first found by the experiment solely.

From 3 to 20 min, both the NBO and sodium concentrations changed negligibly, and the amount of silanol was also almost constant. This is attributed to the higher water resistance of the siloxane network reformed at the glass surface.

Between 20 and 60 min, the sodium ions located near the glass surface slowly diffused into the bulk water to compensate for the concentration gradient of sodium in the water phase.

In summary, we observed sodium leaching and hydroxyl formation during the first 30 s of the glass–water reaction, which is consistent with previous MD simulations. By contrast, during the timescale used for this real experiment, the siloxane network re-formed owing to the dehydration reaction of the silanol groups. The re-formation of the network appeared to stabilize the surface and prevent further corrosion and may be considered "self-healing" of the surface. After 45 min, the number of silanol groups gradually increased. Therefore, a more stable surface should form after the immersion of a glass substrate in water for a few tens of minutes. Consequently, our observations suggest glass durability may be improved by dipping the glass substrates in water after lapping, polishing, and cleaning.

ACKNOWLEDGMENTS

This work was supported by Institute for Nanoscience Design, Osaka University.

Ken-ichi Fukui fukui.ken-ichi.es@osaka-u.ac.jp

ORCID

Katsuaki Miyatani https://orcid.org/0009-0008-4242-3841
Shin-ichi Amma https://orcid.org/0000-0003-3564-1206
Lu Deng https://orcid.org/0000-0002-5912-3908
Madoka Ono https://orcid.org/0000-0002-1216-2731
Shingo Urata https://orcid.org/0000-0001-6878-345X
Jincheng Du https://orcid.org/0000-0003-4805-7498
Ken-ichi Fukui https://orcid.org/0000-0001-8780-5853

REFERENCES

1. Dejneka M, Kiczenski TJ. Display glass. In: Springer handbook of glass. Cham: Springer International Publishing; 2019. p. 1521–53.
2. Varshneya AK. Recent advances in the chemical strengthening of glass. Phys Chem Glasses: Eur J Glass Sci Technol B. 2017;58(4):127–32. https://doi.org/10.13036/17533562.58.4.127
3. Banerjee G, Rhoades RL. Chemical mechanical planarization, historical review and future direction. ECS Trans. 2008;13(4):1–19. https://doi.org/10.1149/1.2912973
4. Cheng SL, Chen WC, Lin PB, Ko CT, Chen YH. A novel application of chemical mechanical polishing for panel level organic and glass substrate 68th Electronic Components and Technology Conference. New York: IEEE; 2018. https://doi.org/10.1109/ECTC.2018.00101
5. Cook LM. Chemical processes in glass polishing. J Non-Crystal Solids. 1990;120(1–3):152–71. https://doi.org/10.1016/0022-3093(90)90200-6
6. Gin S, Collin M, Jollivet P, Fournier M, Minet Y, Dupuy L, et al. Dynamics of self-organization explains passivation of silicate glasses. Nat Commun. 2018;9(2169):1–9.
7. Gin S, Guo X, Delaye JM, Angeli F, Damodaran K, Testud V, et al. Insights into the mechanisms controlling the residual corrosion rate of borosilicate glasses. npj Mater Degrad. 2020;4(1):1–9.
8. Frankel GS, Vienna JD, Lian J, Scully JR, Gin S, Ryan JV, et al. A comparative review of the aqueous corrosion of glasses, crystalline ceramics, and metals. npj Mater Degrad. 2018;2:15.
9. Frankel GS, Vienna JD, Lian J, Guo X, Gin S, Kim SH, et al. Recent advances in corrosion science applicable to disposal of high-level nuclear waste. Chem Rev. 2021;121(20):12327–83. https://doi.org/10.1021/acs.chemrev.0c00990
10. Lanford WA, Davis K, Lamarche P, Laursen T, Groleau R, Doremus RH, et al. Hydration of soda-lime glass. J Non-Crystal Solids.1979;33:249–66. https://doi.org/10.1016/0022-3093(79)90053-X
11. Bunker BC. Molecular mechanisms for corrosion of silica and silicate glasses. J Non-Crystal Solids. 1994;178(4):300–308. https://doi.org/10.1016/0022-3093(94)90708-0
12. Conradt R. Chemical durability of oxide glasses in aqueous solutions: a review. J Am Ceram Soc. 2008;91(3):728–35. https://doi.org/10.1111/j.1551-2916.2007.02101.x
13. Takadama H, Kim HM, Kokubo T, Nakamura T. Mechanism of biomineralization of apatite on a sodium silicate glass: TEM−EDX study in vitro. Chem Mater. 2001;13:1108–13. https://doi.org/10.1021/cm0008718
14. Uchino T, Sakka T, Ogata Y, Iwasaki M. Mechanism of hydration of sodium silicate glass in a steam environment: 29Si

NMR and ab initio Molecular orbital studies. J PhysChem. 1992;96:7308–15.
15. Scholze H. Chemical durability of glasses. J Non-Crystal solids. 1982;52(1–3):91–103. https://doi.org/10.1016/0022-3093(82)90283-6
16. Acocella J, Tomozawa M, Watson EB. The nature of dissolved water in sodium silicate glasses and its effect on various properties. J Non-Crystal Solids. 1984;65(2–3):355–72. https://doi.org/10.1016/0022-3093(84)90058-9
17. Shchukarev A, Rosenqvist J, Sjöberg S. XPS study of the silica-water interface. J Electron Spectrosc Relat Phenom. 2004;137–140:171–76. https://doi.org/10.1016/j.elspec.2004.02.095
18. Jung RK, Jung Y, Choi I, et al. Wet Cleaning by Using Amphoteric Electrolyzed Water for Mask Cleaning, ECS Trans. 2019;92(2):209–19. https://doi.org/10.1149/09202.0209ecst
19. Deng L, Miyatani K, Amma SI, Suehara M, Ono M, Yamamoto Y, et al. Reaction mechanisms and interfacial behaviors of sodium silicate glass in an aqueous environment from reactive force field-based Molecular Dynamics simulations. J Phys Chem C. 2019;123(35):21538–47. https://doi.org/10.1021/acs.jpcc.9b05030
20. Deng L, Miyatani K, Suehara M, Amma S., Ono M., Urata S, et al. Ion-exchange mechanisms and interfacial reaction kinetics during aqueous corrosion of sodium silicate glasses. npj Mater Degrad. 2021;5(1):15. https://doi.org/10.1038/s41529-021-00159-4
21. Hahn SH, van Duin ACT. Surface reactivity and leaching of a sodium silicate glass under an aqueous environment: a ReaxFF molecular dynamics study. J Phys Chem C. 2019;123(25):15606–17. https://doi.org/10.1021/acs.jpcc.9b02940
22. Hahn SH, Rimsza J, Criscenti L, Sun W, Deng L, Du J, et al. Development of a ReaxFF reactive force field for NaSiO x/water systems and its application to sodium and proton self-diffusion. J Phys Chem C. 2018;122(34):19613–24. https://doi.org/10.1021/acs.jpcc.8b05852
23. Kalahe J, Mahadevan TS, Ono M, Miyatani K, Urata S, Du J. Temperature dependence of interfacial reactions of sodium aluminosilicate glasses from reactive molecular dynamics simulations. Appl Surf Sci. 2023;619:156780. https://doi.org/10.1016/j.apsusc.2023.156780
24. Kalahe J, Mahadevan TS, Ono M, Miyatani K, Urata S, Du J. Composition effect on interfacial reactions of sodium aluminosilicate glasses in aqueous solution. J Phys Chem B. 2023;127(1):269–84. https://doi.org/10.1021/acs.jpcb.2c06712
25. Jabraoui H, Gin S, Charpentier T, Pollet R, Delaye J. Leaching and reactivity at the sodium aluminosilicate glass—water interface: insights from a ReaxFF molecular dynamics study. J Phys Chem C. 2021;125(49):27170–84. https://doi.org/10.1021/acs.jpcc.1c07266
26. Dongol R, Wang L, Cormack AN, Sundaram SK. Molecular dynamics simulation of sodium aluminosilicate glass structures and glass surface-water reactions using the reactive force field (ReaxFF). Appl Surf Sci. 2018;439:1103–10. https://doi.org/10.1016/j.apsusc.2017.12.180
27. Yeon J, Chowdhury SC, Gillespie Jr. JW. Hydroxylation and water-surface interaction for S-glass and silica glass using ReaxFF based molecular dynamics simulations. Appl Surf Sci. 2023;608:155078. https://doi.org/10.1016/j.apsusc.2022.155078
28. Guo X, Yuan S, Huang J, Chen C, Kang R, Jin Z, et al. Effects of pressure and slurry on removal mechanism during the chemical mechanical polishing of quartz glass using ReaxFF MD. Appl Surf Sci. 2020;505:144610. https://doi.org/10.1016/j.apsusc.2019.144610
29. Guo X, Huang J, Yuan S, Chen C, Jin Z, Kang R, et al. Effect of surface hydroxylation on ultra-precision machining of quartz glass. Appl Surf Sci. 2020;501:144170. https://doi.org/10.1016/j.apsusc.2019.144170
30. Guo X, Yuan S, Gou Y, Wang X, Guo J, Jin Z, et al. Study on chemical effects of H_2O_2 and glycine in the copper CMP process using ReaxFF MD. Appl Surf Sci. 2020;508:145262. https://doi.org/10.1016/j.apsusc.2020.145262
31. Nguyen VT, Fang TH. Molecular dynamics simulation of abrasive characteristics and interfaces in chemical mechanical polishing. Appl Surf Sci. 2020;509:144676. https://doi.org/10.1016/j.apsusc.2019.144676
32. Brugnoli L, Menziani MC, Urata S, Pedone A. Development and application of a ReaxFF reactive force field for cerium oxide/water interfaces. J Phys Chem A. 2021;125(25):5693–708. https://doi.org/10.1021/acs.jpca.1c04078
33. Brugnoli L, Miyatani K, Akaji M, Urata S, Pedone A. New atomistic insights on the chemical mechanical polishing of silica glass with ceria nanoparticles. Langmuir. 2023;39(15):5527–41. https://doi.org/10.1021/acs.langmuir.3c00304
34. Onodera Y, Takimoto Y, Hijiya H, Taniguchi T, Urata S, Inaba S, et al. Origin of the mixed alkali effect in silicate glass. NPG Asia Mater. 2019;11(1):75. https://doi.org/10.1038/s41427-019-0180-4
35. Shirley DA. High-resolution x-ray photoemission spectrum of the valence bands of gold. Phys Rev B. 1972;5(12):4709–14. https://doi.org/10.1103/PhysRevB.5.4709
36. Nesbitt HW, Bancroft GM, Henderson GS, Ho R, Dalby KN, Huang Y, et al. Bridging, non-bridging and free (O^{2-}) oxygen in Na_2O-SiO_2 glasses: an x-ray photoelectron spectroscopic (XPS) and nuclear magnetic resonance (NMR) study. J Non-Crystal Solids. 2011;357(1):170–80. https://doi.org/10.1016/j.jnoncrysol.2010.09.031
37. Miura Y, Matsumoto S, Nanba T, Akazawa T. X-ray photoelectron spectroscopy of sodium aluminosilicate glasses. Phys Chem Glasses. 2000;41(8):24–31.
38. Gin S, Jollivet P, Barba Rossa G, Tribet M, Mougnaud S, Collin M, et al. Atom-probe tomography, TEM and ToF-SIMS study of borosilicate glass alteration rim: a multiscale approach to investigating rate-limiting mechanisms. Geochim Cosmochim Acta. 2017;202:57–76. https://doi.org/10.1016/j.gca.2016.12.029
39. Mahadevan TS, Du J. Hydration and reaction mechanisms on sodium silicate glass surfaces from molecular dynamics simulations with reactive force fields. J Am Ceram Soc. 2020;103(6):3676–90. https://doi.org/10.1111/jace.17059
40. Crundwell FK. On the mechanism of the dissolution of quartz and silica in aqueous solutions. ACS Omega. 2017;2(3):1116–27. https://doi.org/10.1021/acsomega.7b00019

How to cite this article: Miyatani K, Amma S, Deng L, Kalahe J, Morioka M, Suehara M, et al. Surface characterization of sodium silicate glasses after initial water interaction. J Am Ceram Soc. 2025;e20614. https://doi.org/10.1111/jace.20614